## Atomically precise dopant placement

STM-based hydrogen lithography allows us to write structures and place dopants in the silicon surface with atomic precision [1, 2]. Figure 1 shows a hydrogen terminated Si(001) surface where ~4 hydrogen atoms have been desorbed by pulsing the STM tip voltage thereby exposing the underlying reactive Si bonds. After the surface has been dosed with phosphine gas ($PH_3$) and heated to 350°C, the $PH_3$ molecule dissociates and a single P atom is incorporated into the surface. In addition, the hydrogen atoms from the dissociated $PH_3$ molecule have rebonded to the available free Si bonds reterminating the surface. In such a way we can place the P atoms in the surface with atomic precision.

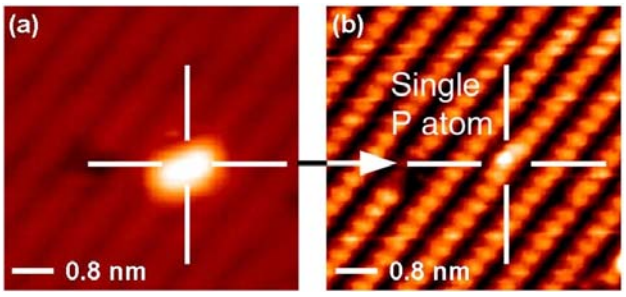


*Figure 1: STM images of atomically precise single P atom placement in silicon. (a) STM image of a hydrogen terminated Si(100) surface with a ~4 hydrogen atoms desorbed by the STM, (indicated by the crosshairs) (b) The same area after $PH_3$ dosing and annealing to 350°C showing a single P atom incorporated at the pre-defined location.*

## Identification of single P atoms in silicon

Before we can position single P atoms in silicon, it is necessary to identify the different P containing surface species that arise from using $PH_3$ gas as the dopant source. To this end we have extensively studied the adsorption and dissociation of $PH_3$ gas on the Si(001) surface using STM imaging and ab-initio theory calculations [3-8]. From these works we have identified the most prominent phosphorus containing species on the surface, see Fig. 2.

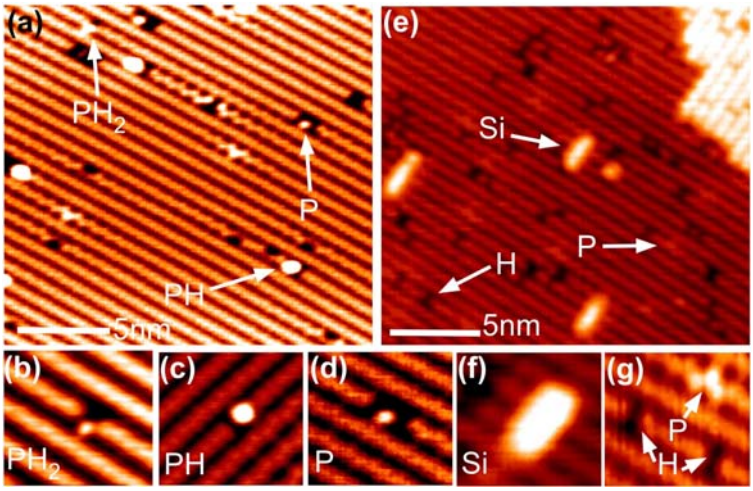


*Figure 2: Identification of atomic-scale P-related features on the silicon surface: (a) a filled state STM image of the Si(100) surface after room temperature dosing with $PH_3$ showing high resolution filled state images of (b) $PH_2$ (c) PH and (d) P fragments on the surface. (e) shows the surface after an anneal to 350°C highlighting (f) the ejected silicon dimer chains and (g) a Si-P heterodimer and two monohydrides on the surface.*

Fig. 2a shows a representative STM image of the Si(001) surface after dosing with a small amount of $PH_3$ displaying numerous different surface species. The most important P-containing surface species on this surface are $PH_2$, PH, and P, shown in Fig. 2b,c, and d respectively. Figure 2e shows a filled state STM image of a Si(001) surface that after dosing with $PH_3$ has been annealed to 350°C. The most prominent feature in this image are the short bright lines, which correspond to rows of Si dimers that have been ejected during the incorporation of phosphorus into the surface. Figure 2f depicts these chains in more detail. In comparison, the incorporated P atom appears rather inconspicuous as a asymmetric, buckled feature (shown in Figure 2g).

In some cases, the differences between the various species in the STM measurements are subtle and can only be resolved by careful voltage-dependent STM imaging. Figure 3a shows filled and empty state STM images of a single P atom incorporated in the Si(001) surface. The structure is sketched on the left. Figure 3b shows the same for a single H atom on the surface, which is often present as a by-product of the $PH_3$ dissociation or remaining from the hydrogen resist layer. The appearance of both features is very similar as expected since they both contain a single Si dangling bond on one side. However, the voltage-dependent STM images reveal small but characteristic differences in the apparent height. The identification of these features in the STM images as either P or H atoms was established by performing experiments with repeated exposures of the surface and comparing the densities of the features after each dosing cycle (Fig. 3c) [8].

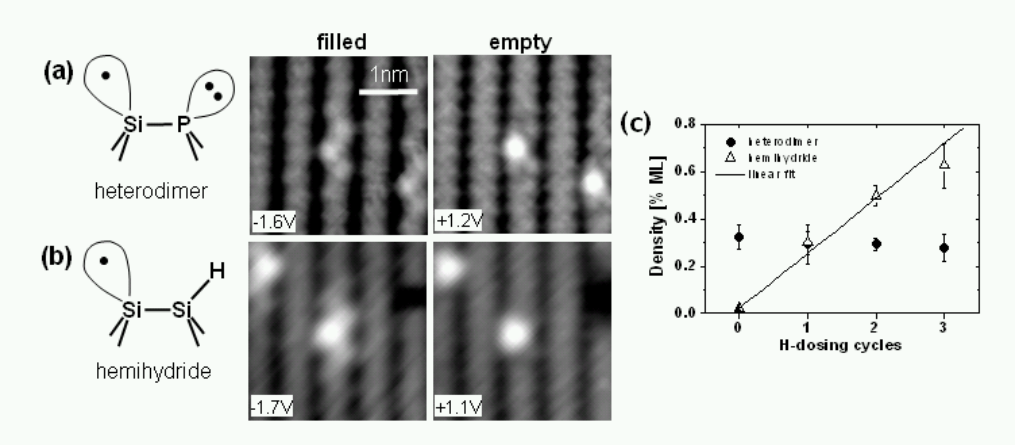


*Figure 3: Experimental distinction between phosphorus and hydrogen atoms on the silicon surface using voltage-dependent STM imaging. (a) Sketch and filled and empty state STM images of the Si-P heterodimer, formed by the incorporation of a P atom into the surface. (b) The same for a Si-Si-H hemohydride, formed by the adsorption of a hydrogen atom to a Si atom in the surface. (c) Statistical analysis leading to the identification of phosphorus and hydrogen in STM images. The surface was prepared with a small amount of phosphorus followed by successive dosing exposures with hydrogen. The features in the STM images were counted according to their appearance and finally assigned to phosphorus or hydrogen based on the expected abundance.*

By performing these combined experimental-theoretical studies we have also gained a thorough understanding of the chemical reaction pathways of $PH_3$ dissociation and P incorporation on the silicon surface. Figure 4 shows three room-temperature STM images (top row) of the step-wise dissociation of a phosphine molecule on Si(001) as it dissociates from $PH_2$+H to PH+2H to P+3H over a period of ~9 min. In the bottom row the chemical structures and formation energies determined from theoretical calculations are presented.

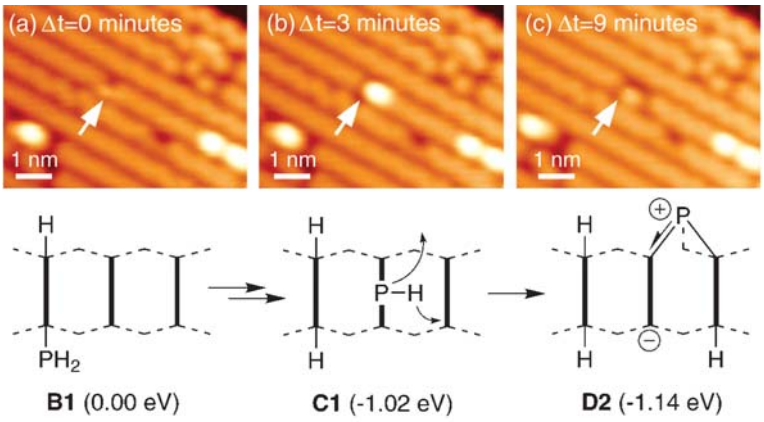


*Figure 4: STM time sequence of images showing the progressive dissociation of $PH_3$ via (a) the asymmetric $PH_2$ structure, (b) the centred PH structure, and (c) the U-shaped P atom before it incorporates into the Si(100) surface. The schematics show the chemical structures together with the formation energies along the dissociation pathway.*

## Electronic structure of single phosphorus atoms in the silicon surface

A single phosphorus atom in a substitutional site on the Si(001) surface forms a Si-P heterodimer. The heterodimer shows a complex and fascinating bias dependence in voltage-dependent STM imaging. We have undertaken detailed theoretical investigations using spin polarized density functional theory calculations. By including the effect of charging the surface we get excellent agreement with the experimental data [9].

In filled state STM images (Fig. 5a) the heterodimer can appear either as a depression or an elevation depending on the bias voltage. The change in appearance can be explained by STM-induced charge transfer into the localized surface states created by the incorporation of the P atom into the surface. Simulated STM images including the charge transfer effect reproduce the trends in the experimental data nicely (Fig. 5b). This charge transfer causes geometric and electronic changes to the Si-P heterodimer (Fig. 5c).

These results highlight that, even under standard imaging conditions, STM can be an invasive probe. This is a crucial point for identifying single atom species and studying reaction pathways with STM.

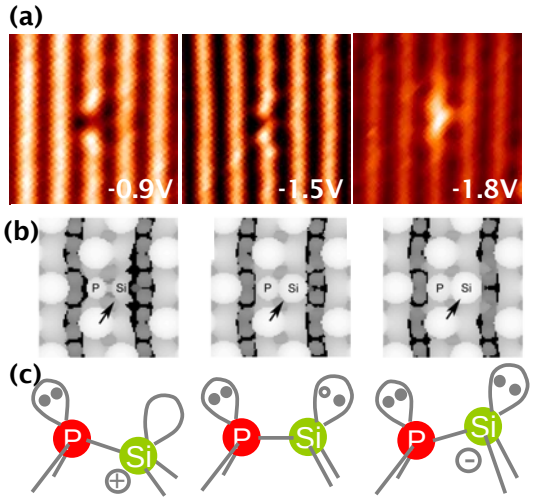


*Figure 5: Changing appearance of a single P atom in the Si(001) surface in STM images with different bias voltages (a) Experimental STM images for different filled state bias. (b) Corresponding simulated STM images. (c) Geometric structure and charge of the Si-P hetero-dimer. Depending on the charge of the heterodimer, the Si atom can be buckled up or down.*

## Removing the hydrogen resist

To provide a robust device the patterned hydrogen resist layer with the P dopants has to be encapsulated with Si. However, the presence of hydrogen on the silicon surface leads to a much rougher surface after Si growth. It is therefore desirable to remove the hydrogen resist layer before Si encapsulation.

We have determined the optimum conditions for thermally removing the hydrogen resist in one step, see Fig. 6 [10]. We have found that a short anneal at 470°C can completely remove the hydrogen resist, while limiting the lateral diffusion to a few nm. For very small structures (< a few nm), we have successfully removed the hydrogen resist using the STM tip reducing the lateral spread of P dopants down to the atomic level.

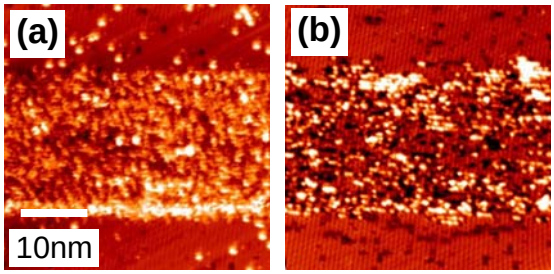


*Figure 6: Removal of the hydrogen resist. (a) STM images of a pattern defined by STM lithography after $PH_3$ dosing and anneally at 350°C to incorporate the P atoms into the silicon surface. (b) STM image of the same area after a short anneal at 470°C which removes the hydrogen with minimal P diffusion out of the STM-patterned region.*

## Buried dopant imaging

One advantage of using STM to pattern devices is that we can image each stage of the fabrication process to see what happens to the dopants. After patterning of the surface with STM (see Fig. 7a), $PH_3$ dosing and P incorporation (Fig. 7b), we encapsulate the P dopants with silicon. To confirm that the P dopants have not moved during encapsulation we image the buried phosphorus atoms underneath the surface. After low-temperature Si growth, buried dopants are hard to distinguish in STM imaging (see Fig. 7c) due to the roughness of the growth surface masking the characteristic dopant patterns in the images. It is however also possible to compensate for the roughness by using current imaging tunneling spectroscopy (CITS) (Fig. 7d) [11]. In this measurement mode, the tip-sample distance is held constant and then an I-V characteristic acquired at each measurement pixel. From these results we can clearly see that the dopants are visible beneath the surface and have not diffused out of the STM-patterned array. It should be noted that whilst it is only possible to image the dopants a few monolayers beneath the surface, the phosphorus atom is unlikely to change its position significantly during further low temperature encapsulation.

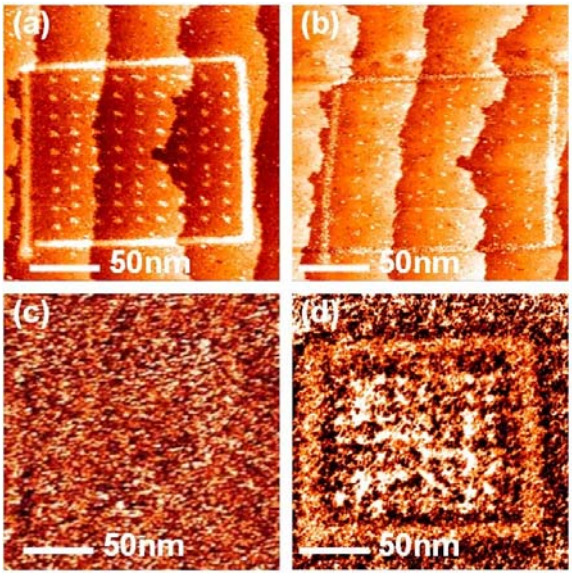


*Figure 7: Preliminary studies of imaging buried dopants. (a) A filled state STM image of a H-terminated Si(100) surface where the STM has been used to remove hydrogen atoms to form an array of desorption sites ~6 nm in diameter surrounded by a box of ~6 nm line width. (b) The same area after $PH_3$ dosing and annealing to 380ºC for 5 min. (c) The same area after encapsulation with 1-2 ML of silicon encapsulation at room temperature and a further anneal at ~380ºC for 5 min. The surface roughness obscures the dopant pattern. (d) An CITS image of the same area, revealing the buried dopant pattern.*


[1] J. L. O'Brien *et al.*, Phys. Rev. B **64**, 161401 (2001)

[2] S. R. Schofield *et al.*, Phys. Rev. Lett. **91**, 136104 (2003)

[3] H.F. Wilson *et al.*, Phys. Rev. Lett. **93**, 226102 (2004)

[4] O. Warschkow *et al.*, Phys. Rev. B **72**, 125328 (2005)

[5] S. R. Schofield *et al.*, J. Phys. Chem. B **110**, 3173 (2006)

[6] O. Warschkow *et al.*, Phys. Rev. B **74**, 195310 (2006)

[7] N. J. Curson *et al.*, Phys. Rev. B **69**, 195303 (2004)

[8] T. C. G. Reusch *et al.*, Surf. Sci. **600**, 318 (2006)

[9] M. W. Radny *et al.*, Phys. Rev. B **74**, 113311 (2006)

[10] T. Hallam *et al.*, Appl. Phys. Lett. **86**, 143116 (2005)

[11] M. Y. Simmons *et al.*, Molecular Simulation **31**, 505 (2005)